

## Two-dimensional indirect excitons in the layer-type trichalcogenide $ZrS_3$

A. Ait-Ouali and S. Jandl

*Département de Physique et Centre de Recherche en Physique du Solide, Université de Sherbrooke, Sherbrooke, Québec, Canada J1K-2R1*

(Received 27 April 1993; revised manuscript received 2 September 1993)

Optical-absorption spectra have been measured near the indirect-gap edge for quasi-one-dimensional  $ZrS_3$  single crystals with chains parallel to the  $b$  axis. The temperature evolution of polarized spectra allows the identification of two indirect parallel gaps ( $E_{\parallel b}$ ) at 2.165 and 2.062 eV with an exciton binding energy of 10 meV and one indirect perpendicular gap ( $E_{\perp b}$ ) at 2.091 eV with an exciton binding energy of 31 meV. While the band-structure model based on the molecular-orbital scheme of the  $(S_2)^{2-}$  molecule is confirmed, the shape analysis of different structures of the absorption coefficient indicates clearly a two-dimensional indirect-band-gap character.

### INTRODUCTION

Low dimensional solids formed by chains or layers of atoms with weak interchain or interlayer bonding are of great interest due to their anisotropic physical properties. From theoretical considerations, Peierls<sup>1</sup> showed in 1955 the inherent instability of one-dimensional metals with respect to periodic lattice distortion at low temperatures. The availability of real materials exhibiting such structural anisotropies caused the surge of recent interest in this area. One-dimensional conductors such as tetrafluoro-tetracyanoquinodimethane (TTF-TCNQ) have been extensively investigated with respect to, among other properties, their charge-density-wave effects.<sup>2</sup> Several one-dimensional insulators such as the  $ABX_3$  exhibit quasi-one-dimensional magnetic behavior.<sup>3</sup>

Trisulfides and triselenides of Ti, Zr, Hf, Nb, and Ta ( $MX_3$ ) constitute a family of structurally related solids. The transition metal forms  $MX_6$  trigonal prisms that share opposite faces resulting in  $MX_3$  chains.<sup>4</sup> The rich variety of physical properties of the various members of this family arises from variations of  $X-X$  and  $M-M$  bonds. Depending on the  $X-X$  bond length, one, two, or three different  $MX_3$  chain-based-structure types are observed.<sup>5</sup>

Transition-metal trichalcogenides of the  $ZrS_3$  family belong to the first group possessing a single type of  $MX_3$  chains,<sup>6</sup> and have been, for over a decade, the subject of intense interest related to their anisotropic character.<sup>7-17</sup> These crystals have a monoclinic-type structure with a symmetry described by the  $C_{2h}^2$  space group. As shown in Fig. 1, the metal ions are located in the center of distorted trigonal prisms which share trigonal faces forming, parallel to the  $b$  axis, chains that are linked together in two-dimensional slabs by the metal-chalcogen bonds. The layers are bound by sulfur-sulfur Van der-Waals interactions.

One of the S-S distances in the  $ZrS_3$  triangular prism base is quite short (2.09 Å) compared to the two others which are considerably larger (3.567 and 3.577 Å),<sup>6</sup> thus provoking the formation of the  $(S_2)^{2-}$  molecule (atoms  $S_{II}$  and  $S_{III}$  of Fig. 1). Accordingly, the formal charges on

the atoms are  $Zr^{4+}$   $(S_2)^{2-}$   $S^{2-}$ . There are two such pairs of close-lying anion atoms, and two more isolated cation atoms around each metal atom. Studies based on x-ray spectroscopy confirmed the  $(S_2)^{2-}$  pairing.<sup>18</sup>

While the phonon behavior in  $ZrS_3$  has been described as quasi-one-dimensional,<sup>7-9</sup> optical dichroism was observed in absorption and reflectivity measurements.<sup>19,20</sup> Jellinek, Pollak, and Shafer<sup>21</sup> assigned the absorption peaks to electronic transitions between the  $\Sigma_g^+$  states and the  $\Pi_u$  states of the  $3p$  levels of the  $(S_2)^{2-}$  ion in terms of a molecular-orbital scheme. Myron, Harmon, and Khumolo<sup>22</sup> predicted an indirect band gap which had been established through absorption by Kurita *et al.*,<sup>23</sup> and temperature-modulated reflectivity by Provencher *et al.*<sup>24</sup>

The shape of absorption spectra in two-dimensional

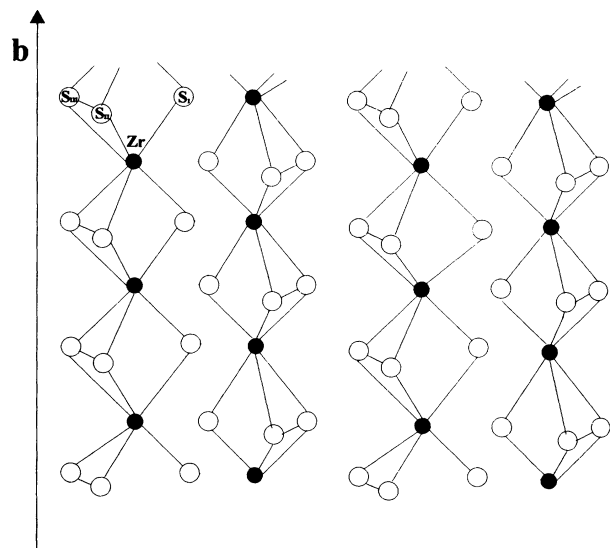


FIG. 1. Crystallographic structure of  $ZrS_3$ -type compounds, illustrating both chain and layer characters. The unit cell contains two  $ZrS_3$  molecular groups located in adjacent chains.

(2D) indirect-gap semiconductor quantum wells has been recently treated theoretically by Basu and Paul<sup>25</sup> for ideal structures. Their main prediction for the absorption coefficient is the existence of step functions representing 2D bound exciton transitions, and of linear variations describing 2D band-band transitions. As also mentioned in their study, comparison with experiment at finite temperature should include a convolution of theoretical spectra with a line-shape function arising from different scattering processes. Moreover, quantitative predictions are not possible even in thoroughly studied indirect-gap quantum wells made of, e.g.,  $\text{Si}_x\text{Ge}_{1-x}$ , since most of the parameters involved in the theoretical expressions remain unknown. Nevertheless,  $\text{ZrS}_3$ , with its electrical and vibrational anisotropic properties, constitutes an ideal candidate for verifying qualitatively theoretical predictions related to electronic behavior in low dimensional systems other than quantum wells.

In this paper we report high-resolution polarized absorption spectra around the indirect-band-gap transitions as a function of temperature, in order to establish the dimensionality of the electronic behavior and the validity of the  $(S_2)^{2-}$  molecular-orbital scheme.

### EXPERIMENT

$\text{ZrS}_3$  single crystals were prepared in sealed quartz ampoules by direct combination of the elements according to the procedure of Ref. 19. All crystals grew in platelets parallel to the  $(a,b)$  plane, and their x-ray spectra confirmed the  $C_{2h}^2$  structure. Typical dimensions of the samples were about  $10\text{mm} \times 2\text{mm} \times 30\mu\text{m}$ .

Polarized absorption spectra were recorded using a Bomem DA3-002 Fourier-transform spectrometer with a quartz beam splitter and a Si detector. Low-temperature measurements were made with the sample mounted in a continuous liquid-helium flow cryostat with light at normal incidence to the  $(a,b)$  crystal plane such that the electric field was either parallel to the  $b$  crystal axis (parallel polarization) or to the  $a$  crystal axis (perpendicular polarization).

### RESULTS AND ANALYSIS

Measurements of absorption and dichroism are shown in Figs. 2, 3(a), and 3(b). Fitting for both polarizations  $\mathbf{E}||\mathbf{b}$  and  $\mathbf{E}\perp\mathbf{b}$  is obtained by adding the predicted two contributions for a two-dimensional indirect-gap semiconductor:<sup>25-27</sup>  $S[h\nu - E_g + R / (n + \frac{1}{2})^2 \pm \hbar\omega_{\text{ph}}]$ , and  $h\nu - E_g \pm \hbar\omega_{\text{ph}}$ , with either phonon absorption (+) or phonon emission (-).  $E_g$  and  $R$  stand for the indirect energy gap and the two-dimensional Rydberg. 3D models, with absorption coefficients of the form  $(h\nu - E_g + R/n^2 \pm \hbar\omega_{\text{ph}})^{1/2}$  and  $(h\nu - E_g \pm \hbar\omega_{\text{ph}})^2$  for excitonic and band-band indirect transitions, respectively, could not reproduce the experimental data due principally to the presence of linear regions that are representative of 2D behavior. Broadening of the excitonic states that can be caused by impurities or defects are taken into account in a phenomenological way by convoluting the  $S$

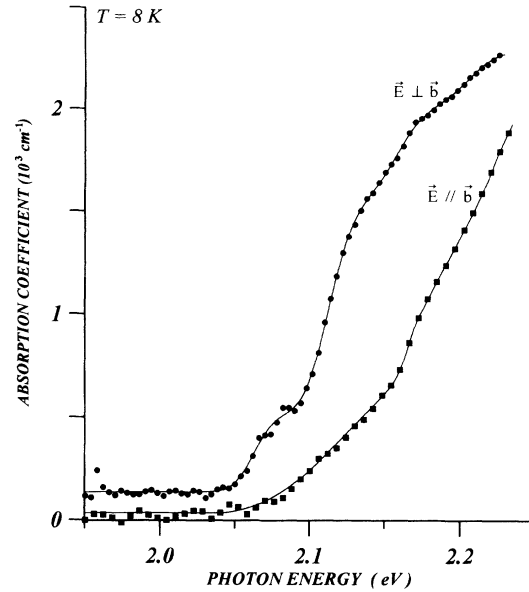


FIG. 2. Polarized spectra near the absorption edge at 8 K. The solid curves correspond to the fit with expressions for the 2D indirect band-band and excitonic transitions. The  $(\mathbf{E}\perp\mathbf{b})$  curve is shifted by  $125\text{ cm}^{-1}$ .

function and the linear function, respectively, with a Gaussian centered at the step energy, and a gate centered at the starting of the linear absorption component.

In Figs. 4(a) and 4(b), evolution with temperature of various absorption energies is shown for  $\mathbf{E}||\mathbf{b}$  and  $\mathbf{E}\perp\mathbf{b}$  within the crystal slabs  $(a,b)$  plane. In the parallel polarization [Fig. 4(a)], exciton transitions at 100 K correspond to phonon absorption  $E_g - E_x - \hbar\omega_{\text{ph}}$  (lines 2 and 3) for the 2.123- and 2.142-eV steps, and to phonon emission  $E_g - E_x + \hbar\omega_{\text{ph}}$  (lines 6 and 4) for the 2.197- and 2.163-eV steps. The deduced zone boundary phonon energies are 11 and 37 meV, and would correspond to phonons observed in Raman spectroscopy<sup>7-17</sup> and infrared measurements.<sup>8,14</sup> In such a low dimensional structure, the dispersion of photon energy is expected to be small. Thus the extrapolated value of  $E_g - E_x$  at 8K becomes 2.155 eV, while the band-band transition  $E_g + \hbar\omega_{\text{ph}}$  (line 5) is 2.176 eV. Consequently, with  $\hbar\omega_{\text{ph}} = 11$  meV, the deduced band-gap energy  $E_g$  and the exciton binding energy  $E_x$  are 2.165 eV and 10 meV, respectively. Line 1, which corresponds to a band-band transition with photon emission has a different temperature dependence. We attribute it to a second gap of 2.062 eV at 8K assuming the 11-meV phonon participation.

In the perpendicular polarization configuration [Fig. 4(b)], lines 1, 2, and 3 correspond to excitonic transitions with phonon absorption, while lines 6, 5, and 4 represent their phonon emission counterpart. The involved phonons have the following energies 99.3, 44.5, and 8.5 meV. At 300 K the band-band transitions  $E_g \mp \hbar\omega_{\text{ph}}$  with phonon absorption (1.974 eV) and emission (2.010 eV) locate the gap energy at 1.992 eV, and, consequently, an exciton binding energy of 31 meV is deduced by considering the exciton transitions located at  $E_g - E_x \pm \hbar\omega_{\text{ph}}$ . Knowing

the energy of the emitted phonons in the excitonic transitions 4, 5, and 6, the extrapolated excitonic gap energy at 8 K is estimated at 2.060 eV, giving a band-gap energy of 2.091 eV. Using  $\epsilon_{\parallel}$  and  $\epsilon_{\perp}$  of Ref. 28, the excitons' effective mass is evaluated and found approximately equal to  $0.04m_e$  for both polarizations.

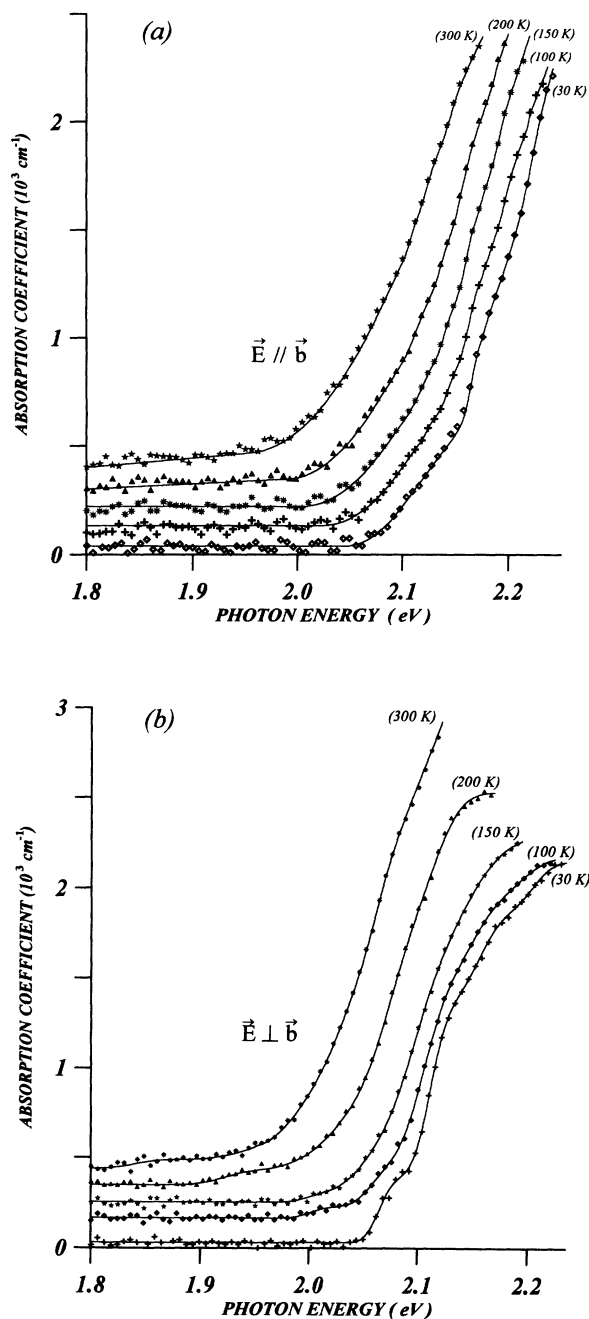


FIG. 3. Temperature dependence of the absorption spectrum near the absorption edge with light polarized parallel (a) and perpendicular (b) to the crystal  $\mathbf{b}$  axis. The solid curves result from the fitting process as in Fig. 2. The vertical axis absorption coefficient values correspond to the 30-K spectrum, while the other spectra are respectively shifted by  $100 \text{ cm}^{-1}$  for clarity.

## DISCUSSION

In summary, we found, in the parallel polarization at 8 K, a first gap at 2.165 eV, with an exciton binding energy of 10 meV and a second gap at 2.062 eV. In the perpendicular polarization, the band-gap energy is 2.091 eV, with an exciton binding energy of 31 meV. This is consistent with the molecular-orbital scheme of the  $(S_2)^{2-}$  molecule<sup>21</sup> that predicts, following a spin-orbit splitting

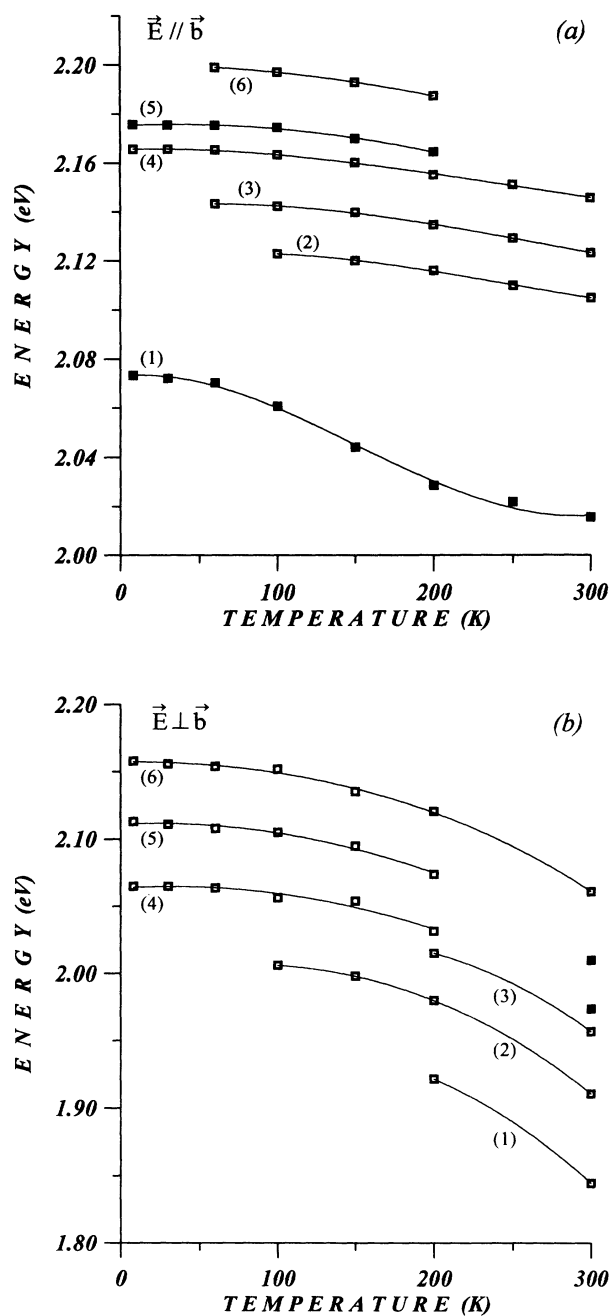


FIG. 4. Energy temperature evolution of the optical transitions for  $\mathbf{E} \parallel \mathbf{b}$  (a) and  $\mathbf{E} \perp \mathbf{b}$  (b). The solid lines are a guide to the eyes. Full and empty squares stand for band-band and excitonic transitions, respectively. The size of the symbols corresponds to the fitting uncertainties.

of the first molecular level, a perpendicular gap slightly above the first parallel gap. The presence of external fields generated by the neighboring atoms does not modify the selection rules for the transitions between the  $(S_2)^{2-}$  molecular levels even if these selection rules hold strictly for the free molecule and dipole radiation.

The binding energy of the exciton associated with the 2.062-eV parallel gap could be obtained from the thermorefectivity measurements reported by Provencher *et al.*<sup>24</sup> From Fig. 3 and Table 1 of their study we deduce that the low-energy structure of 2.050 eV, observed in the parallel polarization, has a different origin because of its small damping parameter once compared to the three other structures. As they reported for this transition, impurities and lattice defects could allow a zero-phonon exciton recombination. The additional broader structure observed at 2.092 eV is an exciton transition with the emission of a phonon of 42 meV. We infer that the other two structures observed at 2.081 and 2.146 eV, in the perpendicular polarization, would correspond to exciton transitions with the emission of two different phonons, because their damping parameters are similar to that of the 2.092-eV parallel structure. Using the value of the band-gap energy at 8 K, and the exciton binding energy of 31 meV, with the fact that the gap decreases by about 2 meV between 8 and 50 K [Fig. 4(b)], the energies of the phonons involved are 23 and 23 + 65 meV. The 23-meV phonon would be the zone-edge mode corresponding to the Raman mode observed at 19 meV, while the 65-meV phonon is the  $(S_2)^{2-}$  Raman-active molecular vibration.

Taking into account the decrease of the gap by about 2 meV between 8 and 50 K, and using the value of 2.050 eV for the exciton band gap,<sup>24</sup> the binding energy of the exciton associated with the 2.062-eV gap value at 8 K is estimated to be 10 meV. This exciton binding energy is the same as the one deduced for the 2.165-eV parallel gap exciton.

Kurita *et al.*<sup>23</sup> have interpreted the absorption edges of their polarized spectra (2.055 eV for  $E\parallel b$ , and 2.085 eV for  $E\perp b$ ) as being non-phonon-assisted transitions, and the two additional observed structures (2.095 eV for  $E\parallel b$ , and 2.13 eV for  $E\perp b$ ) as excitonic transitions with the emission of phonon. Our results confirm their interpretations for the parallel polarization, even though they used a three-dimensional model to fit their data, since the determination of energy thresholds is model independent.

They observed an impurity broad band present at temperatures below 140 K for  $E\parallel b$ , but absent for  $E\perp b$ . These impurities can participate in the absorption process by assisting an exciton transition in the parallel polarization. The energy of such a transition would be the exciton band gap itself around 2.055 eV, close to our deduced value of 2.052 eV. Their association to an impurity-assisted transition at the 2.085-eV threshold, observed in the perpendicular polarization, however, is not justified since the impurity band is absent in this polarization. Using our values for the band-gap energy of 2.091 eV, and for the exciton binding energy of 31 meV, we reinterpret the two thresholds at 2.085 and 2.130 eV as being excitonic transitions, with the emission of two different phonons of energies around 25 and 70 meV.

## CONCLUSION

In this study we present polarized optical-absorption measurements with a detailed analysis of a typical representative of the structural anisotropic  $MX_3$  family. To our knowledge, a two-dimensional behavior in the electronic band structure and its related properties is reported here for the first time for a member of the semiconducting group of this family. In the parallel polarization, two different gaps at 2.165 and 2.062 eV are extracted with an exciton binding energy of 10 meV, while in the perpendicular polarization the gap energy is estimated at 2.091 eV with an exciton binding energy of 31 meV. Previously reported measurements have been partly reinterpreted for the perpendicular polarization. Electronic properties based principally on the molecular-orbital levels of the  $(X_2)^{2-}$  molecule are confirmed, suggesting that future band-structure calculations of the  $MX_3$  semiconducting family should predominantly integrate such a scheme.

## ACKNOWLEDGMENTS

The help of M. Parenteau in fitting the spectra is gratefully acknowledged. One of us (A.A.-O.) acknowledges the financial support of the Algerian government. This work was supported by the Natural Sciences and Engineering Research Council of Canada (NSERC) and the Fonds pour la Formation des Chercheurs et l'Aide à la Recherche of the Government of Québec.

<sup>1</sup>R. E. Peierls, *Quantum Theory of Solids*, (Oxford University Press, Oxford, 1955).

<sup>2</sup>J. T. Devreese, R. Evrard, and U. E. V. Van Doren, *Highly Conducting One-Dimensional Solids* (Plenum, New York, 1979).

<sup>3</sup>See, for example, S. Jandl, M. Banville, Q. F. Xu, and A. Ait-Ouali, *Phys. Rev. B* **46**, 11 585 (1992), and references within.

<sup>4</sup>J. Rouxel, A. Meerschaut, L. Guemas, and P. Gressier, *Ann. Chem. (France)* **7**, 445 (1982).

<sup>5</sup>J. A. Wilson, *Phys. Rev. B* **19**, 6456 (1979).

<sup>6</sup>S. Furuseth, L. Brattås, and A. Kjekshus, *Acta Chem. Scand. A* **29**, 623 (1975).

<sup>7</sup>A. Ait-Ouali, S. Jandl, J. P. Marinier, J. M. Lopez Castillo, and A.-M. S. Tremblay, *Phys. Rev. B* **46** 5183 (1992).

<sup>8</sup>S. Jandl, C. Deville Cavellin, and J.-Y. Harbec, *Solid State Commun.* **31**, 351 (1979).

<sup>9</sup>S. Jandl, M. Banville, and J.-Y. Harbec, *Phys. Rev. B* **22**, 5697 (1980).

<sup>10</sup>T. J. Wieting, A. Grisel, F. Lévy, and Ph. Schmid, in *Quasi-One-Dimensional Conductors I*, Lecture Notes in Physics, Vol. 95 (Springer-Verlag, Berlin, 1979), p. 354.

<sup>11</sup>J.-Y. Harbec, C. Deville Cavellin, and S. Jandl, *Phys. Status Solidi B* **96**, K117 (1979).

<sup>12</sup>C. Deville Cavellin and S. Jandl, *Solid State Commun.* **33**,

- 813 (1980).
- <sup>13</sup>A. Zwick, M. A. Renucci, and A. Kjekshus, *J. Phys. C* **13**, 5603 (1980).
- <sup>14</sup>C. Sourisseau and Y. Mathey, *Chem. Phys.* **63**, 143 (1981).
- <sup>15</sup>A. Grisel, F. Lévy, and T. J. Wieting, *Physica B+C* **99B**, 365 (1980).
- <sup>16</sup>T. J. Wieting, A. Grisel, and F. Lévy, *Physica* **105B**, 366 (1981).
- <sup>17</sup>A. Zwick, M. A. Renucci, R. Carles, N. Saint-Cricq, and J. B. Renucci, *Physica* **105B**, 361 (1981).
- <sup>18</sup>R. Hoffmann, S. Shaik, J. C. Scott, M. H. Whangto, and M. J. Fushee, *J. Phys. C* **3**, 1773 (1983).
- <sup>19</sup>W. Schairer and M. W. Shafer *Phys. Status Solidi A* **17**, 181 (1973).
- <sup>20</sup>F. S. Khumalo, C. G. Olson, and D. W. Lynch, *Physica* **105B**, 163 (1981).
- <sup>21</sup>F. Jelinek, R. A. Pollak, and M. W. Shafer, *Mat. Res. Bull.* **9**, 845 (1974).
- <sup>22</sup>H. W. Myron, B. N. Harmon, and F. S. Khumalo, *J. Phys. Chem. Solids* **42**, 263 (1981).
- <sup>23</sup>S. Kurita, J. L. Staehli, M. Guzzi, and F. Lévy, *Physica* **105B**, 169 (1981).
- <sup>24</sup>R. Provencher, R. Gagnon, S. Jandl, and M. Aubin, *J. Phys. C* **21**, 615 (1988).
- <sup>25</sup>P. K. Basu and Sajal K. Paul, *Phys. Rev. B* **46**, 13 389 (1992).
- <sup>26</sup>K. Nakao, H. Kamimura, and Y. Nishina, *Nuovo Cimento LXIIB*, N. 1, 45 (1969).
- <sup>27</sup>H. Kamimura, K. Nakao, and Y. Nishina, *Phys. Rev. Lett.* **22**, 1379 (1969).
- <sup>28</sup>P.-E. Seguin, M. Poirier, and R. Provencher, *J. Phys. C* **19**, 4303 (1986).